EFFECTS OF SOFT SOIL DEFORMATIONS ON BURIED STRUCTURES DUE TO FAULT DISLOCATION IN BEDROCK

Alireza Farahani [1] , Anil C. Wijeyewickrema [2] and Tatsuo Ohmachi [3]

1) Post Doctoral researcher, farahani@cv.titech.ac.jp
2) Associate Professor, anil@cv.titech.ac.jp
3) Professor, ohmachi@enveng.titech.ac.jp

Center for Urban Earthquake Engineering (CUEE), Tokyo Institute of Technology, O-okayama, Meguro-ku, Tokyo 152-8552, Japan

Abstract

This study concerns simulation of fault rupturing during strong ground motion and the effects of faults on underground structures. The method used here includes four steps. First, a numerical tool is developed to obtain distribution of displacements in an elastic medium. Next step is using a proper technique to apply moving boundaries to this medium to simulate fault dislocation. Additional capabilities are also required to include shear-band propagation in soil layers which are considered in the third step and finally, the applications of this study are discussed.

The soft soil layers are modeled using the Radial Point Interpolation meshfree technique, and the bedrock is modeled with finite elements. When applying dynamic fault dislocation inside the bedrock region using the split-node technique, some parts of this region move upward and push the soft soil layers. The split-node technique is used to introduce a displacement dislocation between adjacent elements.

1. Objective and scope of research

In earthquake engineering one of the most important phenomena is to simulate fault deformation during strong ground motion and investigate the effects of the fault on nearby structures. When an earthquake occurs in an urban area, it is important to measure the ground and soil deformations around faulting zone, because there are many underground facilities and lifelines which can be affected by soil deformation.

The objective of this research is to model upper layer soft soil by mesh free method and then apply a fault deformation at bedrock level to observe the deformation distribution of the upper soil layers and study the effects of the fault on buried structures inside the soil layers (Fig. 1). The Radial Point Interpolation meshfree method is used to model the soil layers because meshfree techniques have shown better results than the conventional Finite Element Method (FEM) for simulating large deformations. This is because of mesh distortion in finite elements due to large deformations (Fig. 2).

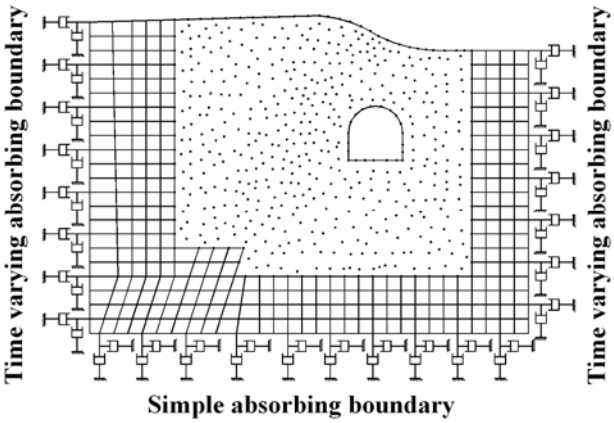

Fig. 1. Dislocation of soft soil layer due to fault dislocation.

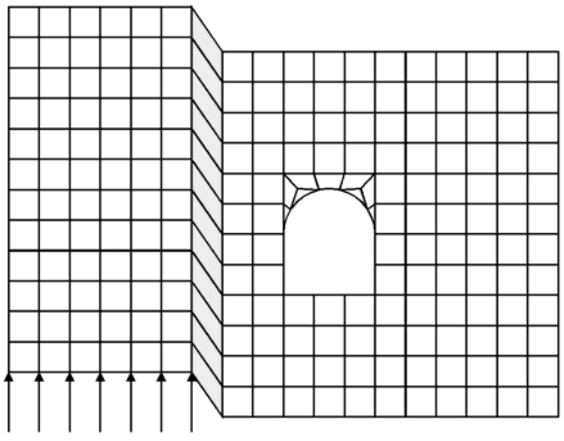

Fig. 2. Element distortion in the elements near fault dislocation.

2. Developing dynamic FEM and Meshfree code

In the conventional FEM method, the medium is descritized by small elements. For each element, all field variables should be calculated at nodal points of the element. In order to calculate these variables, local stiffness, mass and damping matrices should be evaluated at the integration points inside each element and then added together to form the local matrices of that element. These local matrices are calculated using shape functions which relate field variables at the integration points to those of nodal points. Every integration point inside each element is related only to the nodal points of that particular element. Therefore, if the shape of the element is distorted, then those shape functions are not suitable to approximate displacement inside the element any more. This is the origin of the weakness in large deformation using conventional FEM.

Many methods have been developed in different fields of science and engineering to overcome this difficulty. Among them, meshfree technique is a new method. There are different types of meshfree methods. In this research, the kernel of meshfree part of the program is based on Radial Point Interpolation Method (RPIM) which has been developed by Liu and Gu (2001) and Liu and Gu (2005). The reason for choosing RPIM is that it satisfies Kronecker–Delta behavior at nodal points which enables it to be linked to finite element part directly and without any additional treatment.

Using Radial Basis and Polynomial functions, the shape functions are approximated such that they pass through all neighboring nodes at each integration point. Fig. 3 shows a schematic figure of a shape function in RPIM.

The influence of the shape function at each integration point is limited to a small region which is called support domain. Every nodal point inside the support domain has effect on the field variables at the integration point. This is helpful when localized changes of field variables are needed.

In order to calculate the stiffness and mass matrices, the medium is divided into virtual cells which represent the domain of integration. There are several integration points inside every cell at which the stiffness and mass matrices should be evaluated and then added together to form the local matrices of that cell.

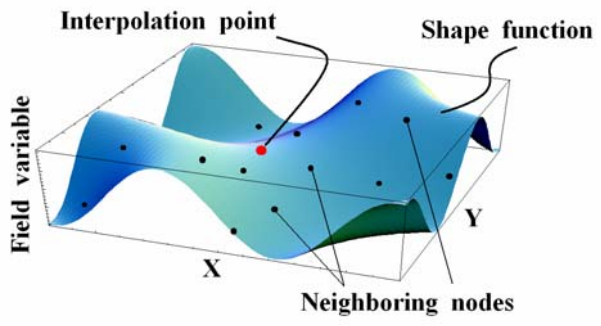

Fig. 3. Shape function of an integration point passing through neighboring nodes.

Next, these local matrices are assembled to form the global stiffness and mass matrices. The remaining procedures for solving governing equations are the same as regular FEM.

Based on the method which was explained in this section, a computer program has been developed.

3. Verification examples for dynamic meshfree code

In order to verify the accuracy and validity of the written code, the following examples of 2D transient wave propagation have been solved and the results were checked with some available time-domain solutions. In the following examples the non-reflecting boundaries are not applied, so, the results are plotted before they are affected by reflected waves from the boundaries.

3.1 Transient response of a massless rigid strip foundation under vertical and horizontal harmonic loads

In this example two-dimensional transient wave propagation due to vibration of a rigid strip foundation under vertical and horizontal harmonic loads is simulated and the results are compared with the results of BEM in time domain (Spyrakos and Beskos 1986). The geometry of the system is shown in Fig. 4.

Material properties of the soil medium are: Modulus of elasticity E = 1.24E10 kg-f/m^2, Poisson's ratio ν = 0.333, mass density ρ = 546.63 kg/m^3, P-wave and S-wave velocities are Vp = 5833.24 m/s and Vs = 2916.62 m/s respectively. This system has been solved for two load cases as:

Case 1: V = 262692 Sin(5814 t) kg-f.

Case 2: H = 262692 Sin(5814 t) kg-f.

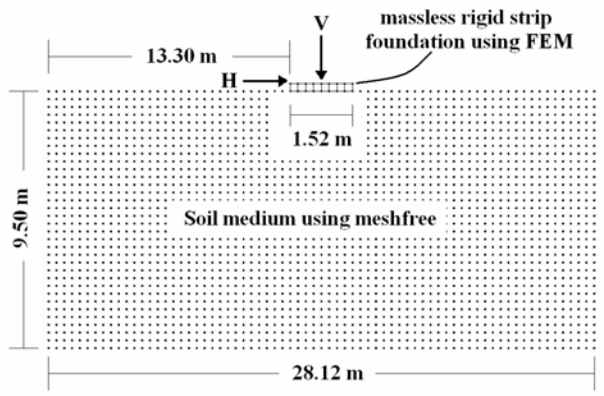

Fig. 4. Geometry of the massless rigid strip foundation system.

Figure 5 shows the vertical displacement of the foundation in Case 1 and Fig. 6 shows the horizontal displacement of the foundation in Case 2.

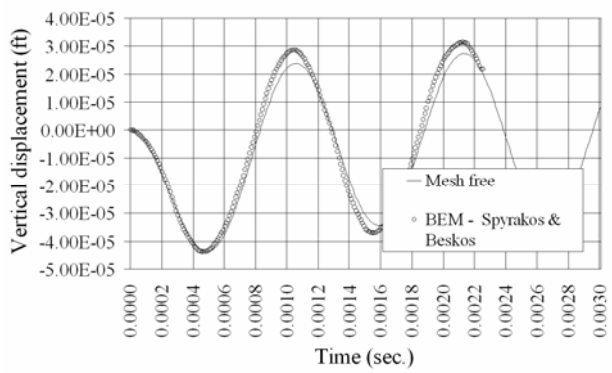

Fig. 5. Vertical displacement of the rigid foundation under vertical harmonic load.

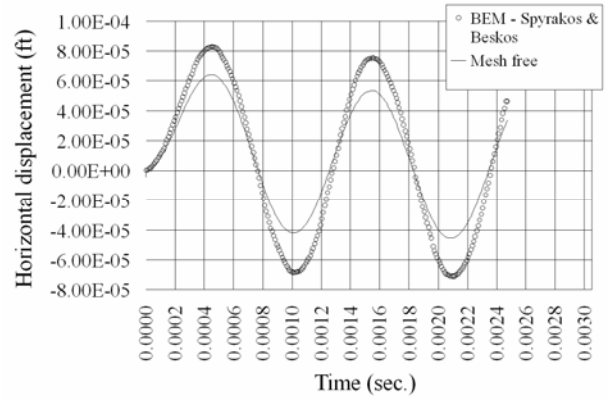

Fig. 6. Horizontal displacement of the rigid foundation under horizontal harmonic load.

Figures 5 and 6 show good agreement between the results of meshfree program and the BEM results.

3.2 Transient response of a massless rigid strip foundation under vertical impulsive load

In order to check the results of the meshfree code for very high frequency transient loading, an impulsive vertical load (Case 3) is applied to the previous system and the vertical displacement of the foundation is compared with BEM result (Fig. 7).

Case 3: V = 262692 kg-f $0 \leq t \leq 0.16E\text{-}4$ sec.

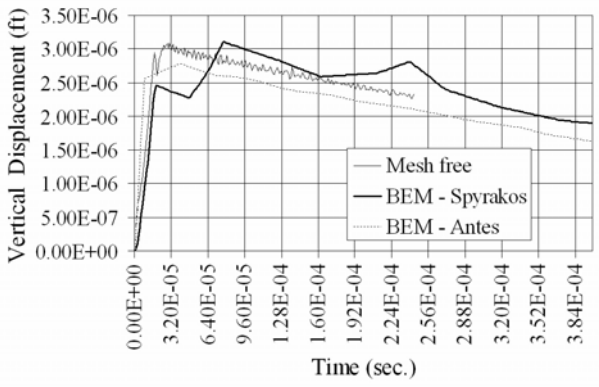

Fig. 7. Vertical displacement of the rigid foundation under vertical impulse load.

It can be seen in Fig. 7 that the meshfree result curve passes between the curves related to two boundary element methods. The good agreement among the results of verification examples of Section 3 shows that the meshfree code is working properly.

4. Simulation of flexible moving boundary

In this section the method of applying fault dislocation is explained. The conventional way of applying fault dislocation at the base of the soil layers is to move the part of the boundary at one side of the fault with prescribed displacement and keep the boundary at the other side of the fault fixed. The weakness of this method is that by applying predefined displacements at the boundary, the nodes of that boundary become rigid such that the incident waves to these boundaries are reflected back to the system again without affecting these boundaries hence this conventional method cannot simulate transmitting boundaries which can be called rigid moving boundary method. To overcome this difficulty, the split-node technique is used to introduce a displacement dislocation between adjacent elements (Melosh and Raefsky 1981). The near field is modeled by meshfree technique and a finite element mesh is linked to this area at the

boundary nodes (Fig. 8). The fault dislocation is applied inside the finite element region, hence, this region deforms. Since the meshfree region and the finite element region share some nodes across their interfaces, the finite element mesh deformations are transferred to meshfree region through these shared nodes. Thus, the moving boundary of meshfree region is modeled by flexible FE mesh which can be called flexible moving boundary.

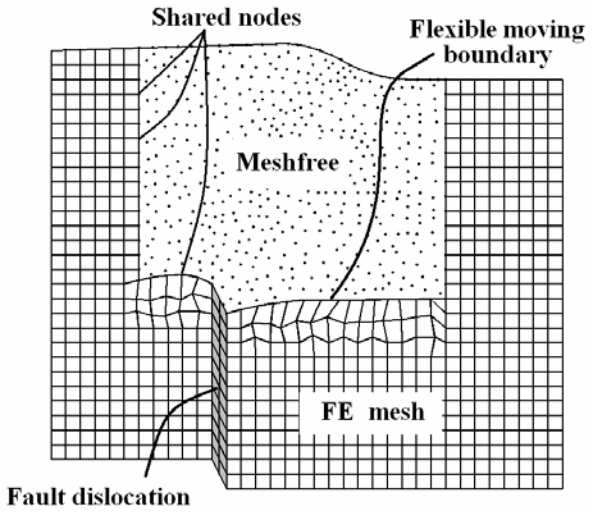

Fig. 8. Simulation of flexible moving boundary using the split–node technique.

In the split–node technique the fault dislocation is replaced by forces which produce the same amount of displacements as the actual fault does. For simplicity only one element on each side of the fault line is depicted in Fig. 9.

Before the faulting the two elements are shown by IMNJ and MKLN. After the fault occurs the two points M and N move to the points M' and N' respectively, but the corners of the two deformed elements on the fault line have some dislocations with respect to M' and N' which are called ΔU_M and ΔU_N respectively.

If stiffnesses of the fault elements are known, then the induced forces in the nodes of the fault elements due to these dislocations can be calculated. Fault elements are the elements which have at least one shared node with the fault line (gray elements in Fig. 8). After calculating these induced forces at fault elements nodes, they are applied to the original model with the opposite sign. These forces produce the same deformations in the system as the fault dislocation does.

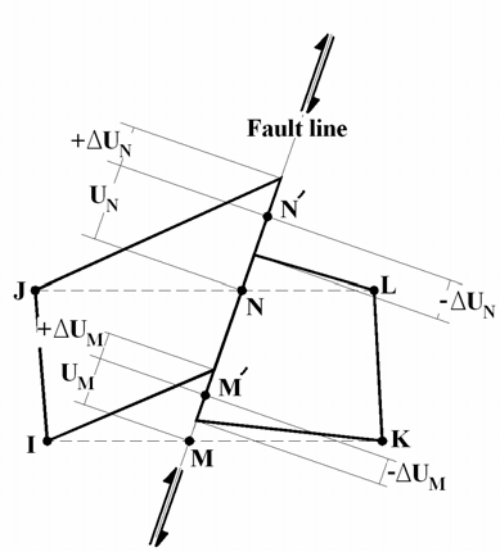

Fig. 9. Deformations of elements at the both sides of fault line.

5. Verification example for split – node technique

The method which was explained in section 4 is the basis of applying fault dislocation by flexible moving boundary. In the next section an example has been solved and verified with the analytical result.

5.1 Vertical Dip–Slip faulting at the surface of a half–plane (static analysis)

In this section the surface deformation of a half–plane due to a vertical dislocation has been obtained and compared with the analytical solution (Freund and Barnett 1976). The geometry of the problem is shown in Fig. 10. Dimensions of each element are 0.1m by 0.1m. Because any material properties can be used, the material properties of the medium are considered to be the same as previous examples. The crack dislocation is considered to be 0.1m at each side.

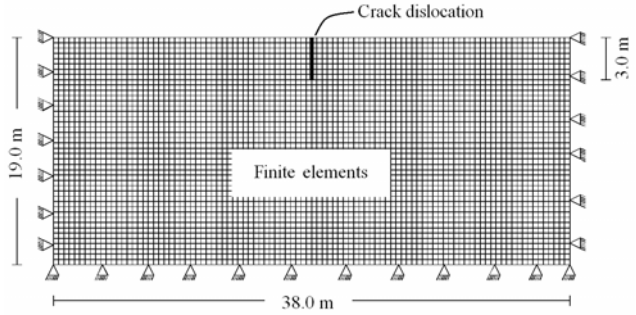

Fig. 10. Geometry of half–plane medium under vertical dislocation.

The surface deformation of the medium around crack is shown in Fig. 11 in more details. There is only one node at each shared point between adjacent elements on the fault line. Although a clear crack can not be seen on this line, still the deformations outside the fault elements are correct.

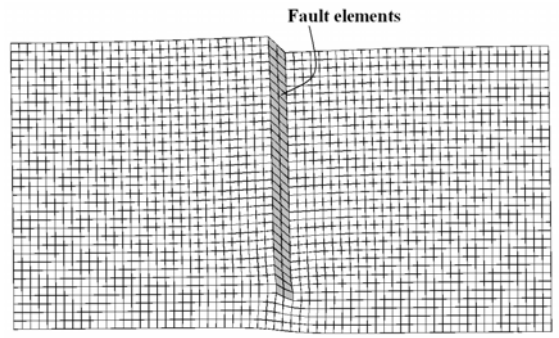

Fig. 11. Deformations of medium around crack

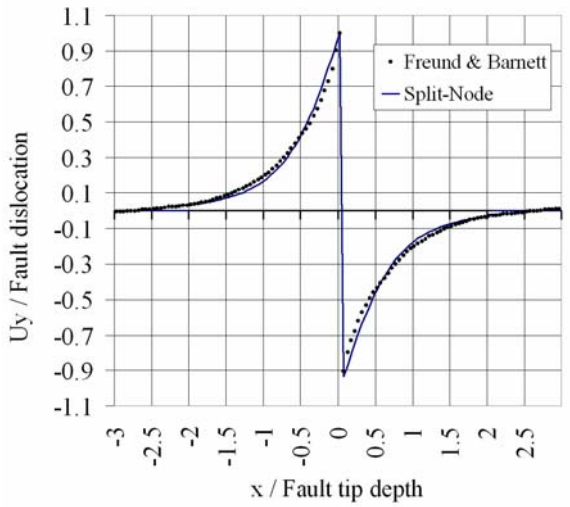

Fig. 12. Normalized vertical surface displacement of the half–plane after faulting.

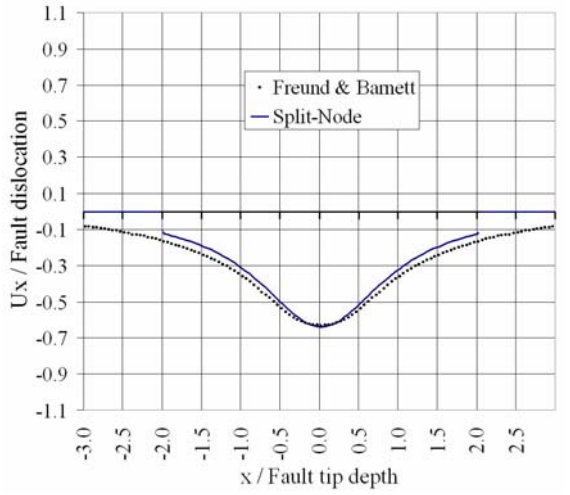

Fig. 13. Normalized horizontal surface displacement of the half–plane after faulting.

In Fig. 12 and Fig. 13, the normalized vertical and horizontal displacements of the surface nodes are drawn respectively. The results show that the kernel for applying fault dislocation at the base of the system, is working properly.

For kinematic source modeling in normal faulting, a source-time function for rupturing should be considered (Haskell 1969). The source–time function represents the fault slip variation in time (Fig. 14).

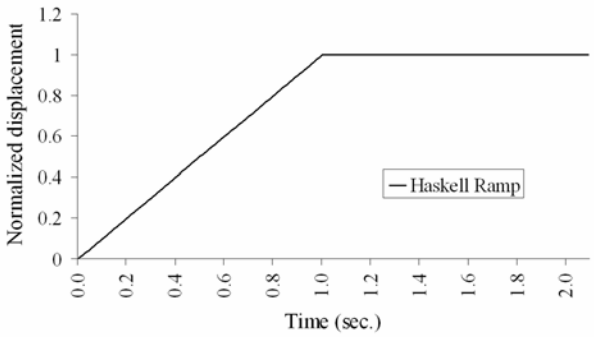

Fig. 14. Simple source – time function used in the kinematic description of faulting.

Using the Haskell ramp function in Fig. 14 for kinematic fault rupturing, the dynamic response of the system can be obtained.

6. Flow chart of progress

All the processes which discussed in this study have been carried out from October 1, 2005 until February 28, 2006. Figure 15 shows the progress and research work completed in this period (gray boxes). During this period a Meshfree-FEM code for the analysis of linear elastic media has been developed and verified with some available solutions for 2D transient wave propagation. The step one and two completed and some part of step three has been done. Step four is the objective of this study.

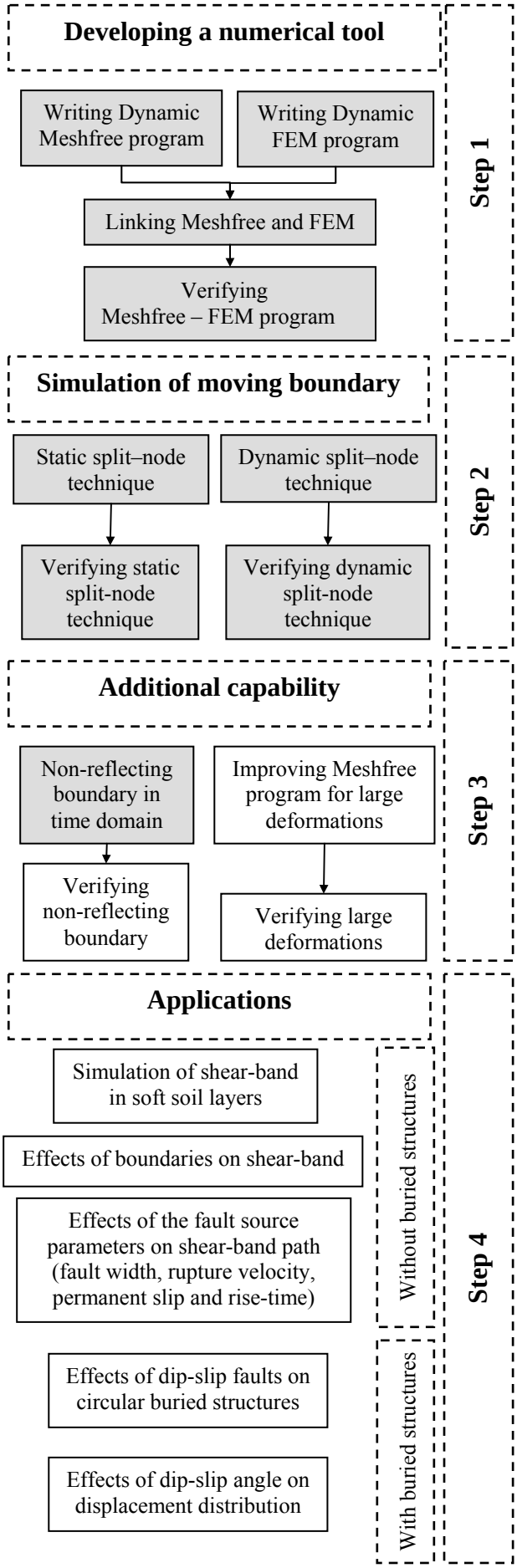

Fig. 15. Flow chart of progress.

7. References

Freund, L. B. & Barnett, D. M. (1976), "A two-dimensional analysis of surface deformation due to Dip-Slip faulting," *Bulletin of the Seismological Society of America*, Vol. 66, No. 3, 667–675.

Haskell, N. A. (1969), "Elastic displacements in the near-field of a propagating fault," *Bulletin of the Seismological Society of America*, Vol. 59, No. 2, 865–908.

Liu, G. R. & Gu, Y. T. (2001), "A point interpolation method for two-dimensional solids," *International Journal for Numerical Methods in Engineering*, Vol. 50, 937–951.

Liu, G. R. & Gu, Y. T. (2005), "An introduction to meshfree methods and their programming," Springer.

Melosh, H. J. & Raefsky, A. (1981), "A simple and efficient method for introducing faults into finite element computations," *Bulletin of the Seismological Society of America*, Vol. 71, No. 5, 1391–1400.

Spyrakos, C. C. & Beskos, D. E. (1986), "Dynamic response of rigid strip-foundations by a time-domain boundary element method," *International Journal for Numerical Methods in Engineering*, Vol. 23, 1547–1565.